

# Three-Dimensional Frameworks Based on Dodecanuclear Dy–hydroxo Wheel Cluster with Slow Relaxation of Magnetization

Yi-Xia Ren,<sup>†,‡</sup> Xiang-Jun Zheng,<sup>\*,†</sup> Li-Cun Li,<sup>\*,§</sup> Da-Qiang Yuan,<sup>||</sup> Miao An,<sup>‡</sup> and Lin-Pei Jin<sup>†</sup>

<sup>†</sup>Beijing Key Laboratory of Energy Conversion and Storage Materials, College of Chemistry, Beijing Normal University, Beijing, 100875, P. R. China

<sup>‡</sup>College of Chemistry and Chemical Engineering, Shaanxi Key Laboratory of Chemical Reaction Engineering, Yan'an University, Yan'an 716000, P. R. China

<sup>§</sup>College of Chemistry, Nankai University, Tianjin 300071, P. R. China

<sup>||</sup>State Key Laboratory of Structural Chemistry, Fujian Institute of Research on the Structure of Matter, Chinese Academy of Sciences, Fuzhou, Fujian 350002, P. R. China

## Supporting Information

**ABSTRACT:** Two new heterometallic coordination polymers,  $[\text{Na}_4\text{Ln}_{12}(\text{stp})_8(\text{OH})_{16}(\text{H}_2\text{O})_{12}] \cdot 10\text{H}_2\text{O}$  [ $\text{Ln} = \text{Dy}$  (**1**) and  $\text{Ho}$  (**2**)], have been prepared from monosodium 2-sulfoterephthalate ( $\text{NaH}_2\text{stp}$ ), dysprosium acetate, or holmium acetate. They are isostructural, possessing a  $[\text{Ln}_{12}(\mu_3\text{-OH})_{16}]^{20+}$  wheel-cluster core based on four vertex-sharing cubane-like  $[\text{Ln}_4(\mu_3\text{-OH})_4]^{8+}$  units. The  $\text{Ln}_{12}$  cores are linked by stp ligands into a three-dimensional (3D) architecture. Magnetic studies indicate that complex **1** exhibits slow relaxation of magnetization, and it can be regarded as the first 3D coordination assembly of a  $\text{Dy}_{12}$  cluster single-molecule magnet.

As a type of new species, polynuclear lanthanide complexes have been attractive for their charming structural features and peculiar potential applications in the fields of catalysis,<sup>1</sup> magnetism,<sup>2</sup> photoluminescence,<sup>3</sup> and absorption of gas.<sup>4</sup> High coordination numbers and large ionic radii of lanthanide ions result in the structural complication and varieties of polynuclear lanthanide complexes. The hydroxyl group plays a crucial role in the formation of the species because it may be the shortest linker for lanthanide ions with  $\mu_2$ -,  $\mu_3$ -, and  $\mu_4$ -bridging fashion.<sup>5</sup> Many such lanthanide hydroxyl complexes featuring different polynuclear lanthanide geometries have been reported, for instance, a  $\text{Ln}_4$  square-shaped cyclic core or cubane-like unit, a  $\text{Ln}_6$  octahedral structure,  $\text{Ln}_7$  and  $\text{Ln}_8$  bis-cubane units, a  $\text{Ln}_{12}$  four vertex-sharing cubane-like unit, a  $\text{Ln}_{15}$  five vertex-sharing cubane-like unit, and even  $\text{Ln}_{26}$  cage-shaped clusters.<sup>6</sup> For the  $\text{Ln}_{12}$  cluster based on a vertex-sharing cubane-like unit, only discrete structures were reported.<sup>6c,d</sup>

Recently, slow relaxation and quantum tunneling of magnetization of single-molecule magnets (SMMs) have inspired exploration of the magnetic properties of polynuclear lanthanide complexes, especially  $\text{Dy}^{3+}$  complexes<sup>7</sup> because of the strong magnetic anisotropy of lanthanides. The slow magnetic relaxations were observed not only in mononuclear lanthanide complexes<sup>8</sup> but also in polynuclear 4f or 3d–4f discrete complexes.<sup>9</sup> The three-dimensional (3D) lanthanide coordination polymers or lanthanide–organic frameworks have been

reported widely; however, 3D structures possessing SMM behavior are scarce. To the best of our knowledge, the reported SMMs based on  $\text{Dy}_{12}$  clusters are discrete.<sup>6c,d</sup> To explore the 3D SMMs, there must be more significant research for their complicated structures, magnetic properties, and potential applications.

We prepared two 3D lanthanide hydroxo frameworks based on dodecanuclear dysprosium/holmium(III) hydroxo cluster cores,  $[\text{Ln}_{12}(\mu_3\text{-OH})_{16}]^{20+}$ , which were assembled into 3D frameworks via  $\mu_3$ -2-sulfoterephthalate (stp) ligands and  $\text{Na}^+$  template ions. Notably, the dysprosium complex exhibits slow relaxation of magnetization, which can be regarded as the first 3D coordination assembly of  $\text{Dy}_{12}$  cluster SMMs.

Hexagonal crystals of  $[\text{Na}_4\text{Ln}_{12}(\text{stp})_8(\text{OH})_{16}(\text{H}_2\text{O})_{12}] \cdot 10\text{H}_2\text{O}$  [ $\text{Ln} = \text{Dy}$  (**1**) and  $\text{Ho}$  (**2**)] were obtained by the hydrothermal reaction of  $\text{Ln}(\text{OAc})_3$ ,  $\text{NaOAc}$ , and  $2\text{-NaH}_2\text{stp}$  in water at 180 °C for 3 days. Single-crystal X-ray diffraction analyses indicated that compounds **1** and **2** are isomorphous. They possess porous frameworks based on  $\text{Ln}_{12}$  cores, with the  $\text{Na}^+$  ions and the water molecules occupying the channels. Herein, only the structure of **1** will be described in detail. In the asymmetrical unit, there are three  $\text{Dy}^{3+}$  ions, one  $\text{Na}^+$  ion, two  $\text{stp}^{3-}$  anions, four  $\text{OH}^-$  anions, three coordination water molecules, and two and a half lattice water molecules. All four crystallographically independent  $\text{Dy}^{3+}$  ions ( $\text{Dy1}$ ,  $\text{Dy2}$ ,  $\text{Dy3}$ , and  $\text{Dy4}$  in Figure 1a) of **1** are in the distorted eight-coordinated anti-square-prism geometry, as shown in Figure S1 in the Supporting Information (SI). They are coordinated by oxygen atoms from  $\text{stp}^{3-}$  anions,  $\text{OH}^-$  anions, and water molecules. Two  $\text{Na}^+$  ions ( $\text{Na1}$  and  $\text{Na2}$ ) lie in different environments:  $\text{Na1}$  is in a five-coordinated trigonal-bipyramidal configuration with two sulfonate oxygen atoms of two  $\text{stp}^{3-}$  anions and three oxygen atoms from water molecules, while  $\text{Na2}$  exists in a square-shaped geometry constructed by two carboxyl oxygen atoms and two hydroxyl atoms with weak coordination interaction (the bond lengths of  $\text{Na2-O11}$  and  $\text{Na2-O15}$  are 2.626 and 2.874 Å, respectively; Figure S2 in the SI). The  $\text{stp}^{3-}$  ligand adopts two

Received: August 21, 2014

Published: November 13, 2014

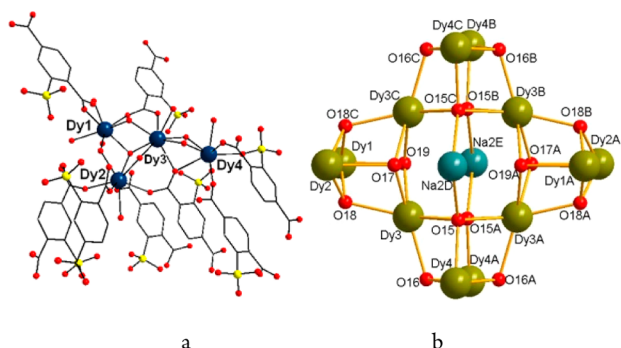


**Figure 1.** (a) Coordination environment of four  $\text{Dy}^{3+}$  ions in **1**. (b)  $[\text{Dy}_{12}(\mu_3\text{-OH})_{16}]^{20+}$  cluster core showing the lantern-like cage formed by two Na ions and the central  $\text{Dy}_4\text{O}_8$  atoms. Symmetry operation: (A)  $1-x, y, -z$ ; (B)  $1-x, 2-y, -z$ ; (C)  $x, 2-y, z$ ; (D)  $1.5-x, 0.5+y, -z$ ; (E)  $-0.5+x, 0.5+y, z$ .

different kinds of  $\mu_5$ -coordinated fashions connecting four  $\text{Dy}^{3+}$  ions and one  $\text{Na}^+$  ion, as shown in Scheme S1 in the SI.

As shown in Figure 1b, the Dy1, Dy2, and two Dy3 ions are bridged by four  $\mu_3$ -OH groups (O17, O18, O19, and O18C) into a cubane-like unit, similar to the cubic unit based on two Dy4 and two Dy3 ions. Such four cubane-like  $[\text{Dy}_4(\mu_3\text{-OH})_4]^{8+}$  units are linked by Dy3 knots end to end into a vertex-sharing dodecanuclear core. Two  $\text{Na}^+$  ions (Na2D and Na2E) together with the central Dy3, O15, O17, and O19 form a  $\text{Dy}_4\text{O}_8\text{Na}_2$  lantern-like cage with a cavity of  $3.75 \times 3.96 \times 2.54$  Å. The adjacent dodecanuclear cores are linked along the  $c$  axis by two  $\mu_2$ -oxygen atoms (O21) from water molecules coordinating with the Dy1 ions (the bond length of Dy1–O21 is 2.455 Å) into a one-dimensional (1D) chain (Figure 2).

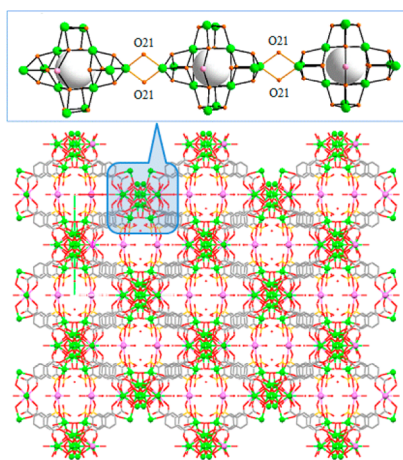


**Figure 2.** 3D metal–organic framework of **1**, showing a 1D chain formed by  $\text{Dy}_{12}$  units along the  $c$  axis.

For the hydroxyl group in complex **1**, there are two coordination modes:  $\mu_3$ - and  $\mu_4$  bridges. Only one hydroxyl (O15) acts as  $\mu_4$  bridge, linking Dy3, Dy4, Dy3A, and Na2D. The other hydroxyl (O16, O17, O18, and O19) acts as  $\mu_3$  bridge, linking three  $\text{Dy}^{3+}$  ions. For coordination water molecules, only O21 acts as a  $\mu_2$  bridge, and the other water molecules (O20, O22, O23, O24, and O25) are terminally coordinated. The  $\text{stp}^{3-}$  ligand serves as a multidentate ligand in a  $\mu_5$ -coordinated fashion and bridges these 1D dodecanuclear chains into a 3D framework in four directions through the oxygen atoms of the carboxyl and sulfonate groups of the  $\text{stp}^{3-}$  ligands (Figure 2). From the  $c$  axis,

there are 1D channels based on these 1D dodecanuclear chains and  $\text{stp}^{3-}$  ligands, in which  $\text{Na}^+$  ions (Na1) and coordination and lattice water molecules are filled in. The  $\text{Na}^+$  ions (Na1) as a template in the channels are coordinated by extending the oxygen atoms (O7) from the sulfonate groups of the  $\text{stp}^{3-}$  ligands. The total void volume,  $V_{\text{void}}$ , within complex **1** without the fillings is 25% per unit volume, as determined by PLATON.<sup>10</sup>

In order to classify the topology of the network, suitable nodes should be defined. The dodecanuclear  $\text{Dy}_{12}$  cluster is considered to be a 20-connected node surrounded by 16  $\text{stp}$  ligands and four  $\mu_2$ - $\text{H}_2\text{O}$  molecules. The  $\text{stp}$  ligand connected to two  $\text{Dy}_{12}$  clusters can be considered a 2-connected node. The ligand  $\mu_2$ - $\text{H}_2\text{O}$  linking two  $\text{Dy}_{12}$  clusters is considered to be a 2-connected node. Figure S3 in the SI shows the topological diagram.

The phase purity of **1** was confirmed by powder X-ray diffraction, as shown in Figure S4 in the SI. Considering the longer lifetime luminescence of the  $\text{Dy}^{3+}$  ion, the luminescent property of **1** was investigated in the solid state at room temperature. As shown in Figure S5 in the SI, its emission spectrum exhibited the characteristic narrow bands (481, 543, 589, 633, and 697 nm) arising from the  ${}^4\text{F}_{9/2} \rightarrow {}^6\text{H}_{15/2}$ ,  ${}^4\text{F}_{9/2} \rightarrow {}^6\text{H}_{13/2}$ ,  ${}^4\text{I}_{15/2} \rightarrow {}^6\text{H}_{11/2}$ ,  ${}^4\text{F}_{9/2} \rightarrow {}^6\text{H}_{11/2}$ , and  ${}^4\text{I}_{15/2} \rightarrow {}^6\text{H}_{9/2}$  transitions of the  $\text{Dy}^{3+}$  ion when excited at 392 nm.

The temperature dependence of the magnetic susceptibility of complex **1** has been carried out in the range 2–300 K under an external magnetic field of 1 kOe. The plot of  $\chi_{\text{M}}T$  (with  $\chi_{\text{M}}$  being the magnetic susceptibility per lanthanide ion) versus  $T$  is shown in Figure 3. The  $\chi_{\text{M}}T$  value at 300 K is  $166.52 \text{ cm}^3 \text{ K mol}^{-1}$ , which

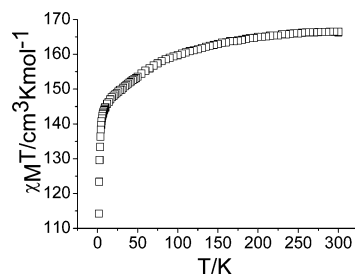


**Figure 3.**  $\chi_{\text{M}}T$  versus  $T$  plot for the dysprosium complex.

is slightly lower than the expected value of  $170.04 \text{ cm}^3 \text{ K mol}^{-1}$  for noncoupling spins of 12  $\text{Dy}^{3+}$  ( $S = 5/2$ ,  $L = 5$ ,  $g = 4/3$ ,  ${}^6\text{H}_{15/2}$ , and  $C = 14.17 \text{ cm}^3 \text{ K mol}^{-1}$ ) but consistent with the data reported in the literature.<sup>11</sup> With decreasing temperature, the  $\chi_{\text{M}}T$  value continuously decreases to reach a value of  $114.24 \text{ cm}^3 \text{ K mol}^{-1}$  at 2.0 K. The overall behavior can be ascribed to depopulation of the  $\text{Dy}^{3+}$  Stark sublevels as well as the exchange interactions between the  $\text{Dy}^{3+}$  ions. The field-dependent magnetization at 2.0 K is shown in Figure S6 in the SI. The magnetization reveals a rapid increase at low field and reaches  $63.44 \text{ N}\beta$  at 7 T, in good agreement with the expected value of  $62.76 \text{ N}\beta$  ( $12 \times 5.23 \text{ N}\beta$ ) for 12 noninteracting  $\text{Dy}^{3+}$  ions, assuming the presence of considerable ligand-field effects.<sup>12</sup> However, no saturation is achieved, which indicates the presence of magnetic anisotropy and/or low-lying excited states in the system.

To study the spin dynamics, alternating-current (ac) magnetic susceptibilities were measured under a zero direct-current (dc) field with an ac field of 2.5 Oe with oscillating frequencies. As shown in Figure 4, both in-phase ( $\chi'$ ) and out-of-phase ( $\chi''$ ) signals show frequency-dependent peak maxima, typical of slow magnetic relaxation. The magnetization relaxation time ( $\tau$ ) is plotted as a function of  $1/T$  in Figure S7 in the SI. Fitting to the

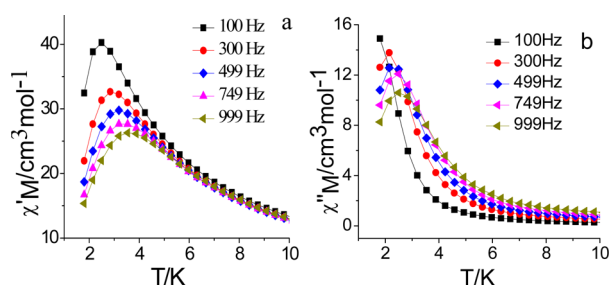


**Figure 4.** Temperature dependence of the in-phase (a) and out-of phase (b) ac susceptibility of the dysprosium complex in a zero dc magnetic field.

Arrhenius law,  $\tau = \tau_0 \exp(\Delta_\tau/kT)$ , afforded an energy gap ( $\Delta_\tau$ ) of 13.66 K and a preexponential factor ( $\tau_0$ ) of  $8.82 \times 10^{-7}$  s ( $R = 0.999$ ), which is in agreement with the expected characteristic relaxation time of  $10^{-6}$ – $10^{-11}$  s for SMMs.<sup>13</sup> The obtained anisotropic energy barrier is comparable to those previously reported for dysprosium-based metal–organic frameworks.<sup>14</sup> The frequency dependencies of the ac susceptibilities were measured at 2.0 and 2.5 K, respectively. The data plotted as Cole–Cole plots show a quasi-semicircular shape (Figure S8 in the SI), and these can be fitted to the generalized Debye model with  $\alpha = 0.29$  and 0.27, indicating the presence of a wide distribution of relaxation time in the dysprosium complex.<sup>15</sup>

For lanthanide-based compounds, slow magnetic relaxation is often attributed to single-ion behavior due to weak exchange interactions between the lanthanide ions, in which the symmetry of the local crystal field around the lanthanide ions plays a critical role. Regarding this, all dysprosium ions are in an approximately square-antiprismatic environment in complex **1**, as in other well-known dysprosium complexes with SMM behavior; thus, magnetic relaxation of **1** is mainly ascribed to the dysprosium ion behavior. Noticeably, the weak Dy–Dy exchange coupling transmitted by the OH group may play an important role in magnetic relaxation because it can suppress the quantum tunneling of magnetization. As shown in the structure, the complex is composed of large Dy<sub>12</sub> cluster units, which can be regarded as the fusion of four vertex-sharing cubane-like Dy<sub>4</sub> units. Thus, this dysprosium derivative can be regarded as the first 3D coordination assembly of Dy<sub>12</sub> cluster SMMs.

In summary, two novel isomorphous lanthanide complexes based on the cluster  $[\text{Ln}_{12}(\mu_3\text{-OH})_{16}]^{20+}$  have been obtained. The dodecanuclear cluster consists of four vertex-sharing cubane-like clusters. The Ln<sub>12</sub> clusters are linked by  $\mu_2$ -H<sub>2</sub>O and stp ligands to 3D metal–organic frameworks with 1D channels. In the channels, Na<sup>+</sup> ions and lattice water molecules are located. The magnetic property of **1** exhibits slow relaxation of magnetization, and all Dy<sup>3+</sup> ions are in an approximately square-antiprismatic environment, as in other well-known dysprosium complexes with SMM behavior, so the title dysprosium complex can be regarded as the first 3D coordination assembly of Dy<sub>12</sub> cluster SMMs.

## ■ ASSOCIATED CONTENT

### 📄 Supporting Information

X-ray crystallographic data in CIF format, detailed experimental procedures, powder X-ray diffraction pattern, emission spectrum, and additional structural and magnetic data for complex **1**. This material is available free of charge via the Internet at <http://pubs.acs.org>.

## ■ AUTHOR INFORMATION

### Corresponding Authors

\*E-mail: xjzheng@bnu.edu.cn.

\*E-mail: llicun@nankai.edu.cn.

### Notes

The authors declare no competing financial interest.

## ■ ACKNOWLEDGMENTS

This work is supported by the Natural Scientific Research Foundation of Shaanxi Provincial Science and Technology Office of China (Grant 2013KRM29-02).

## ■ REFERENCES

- (1) (a) Gandara, F.; Gutierrez-Puebla, E.; Iglesias, M.; Snejko, N.; Monge, M. A. *Cryst. Growth Des.* **2010**, *10*, 128–134. (b) Sheng, H.; Xu, F.; Yao, Y.; Zhang, Y.; Shen, Q. *Inorg. Chem.* **2007**, *46*, 7722–7724.
- (2) (a) Chandrasekhar, V.; Bag, P.; Colacio, E. *Inorg. Chem.* **2013**, *52*, 4562–4570. (b) Anwar, M. U.; Dawe, L. N.; Tandon, S. S.; Bunge, S. D.; Thompson, L. K. *Dalton Trans.* **2013**, *42*, 7781–7794.
- (3) Li, X. L.; He, L. F.; Feng, X. L.; Song, Y.; Hu, M.; Han, L. F.; Zheng, X. J.; Zhang, Z. H.; Fang, S. M. *CrystEngComm* **2011**, *13*, 3643–3645.
- (4) Zhang, B.; Zheng, X. D.; Su, H.; Zhu, Y.; Du, C. X.; Song, M. P. *Dalton Trans.* **2013**, *42*, 8571–8574.
- (5) (a) Sang, R. L.; Xu, L. *Chem. Commun.* **2013**, *49*, 8344–8346. (b) Zheng, Y.; Zhang, Q. C.; Long, L. S.; Huang, R. B.; Muller, A.; Schnack, J.; Zheng, L. S.; Zheng, Z. P. *Chem. Commun.* **2013**, *49*, 36–38.
- (6) (a) Ke, H. S.; Gamez, P.; Zhao, L.; Xu, G. F.; Xue, S. F.; Tang, J. K. *Inorg. Chem.* **2010**, *49*, 7549–7557. (b) Gu, X. J.; Xue, D. F. *Inorg. Chem.* **2007**, *46*, 3212–3216. (c) Wang, R. Y.; Selby, H. D.; Liu, H.; Carducci, M. D.; Jin, T. Z.; Zheng, Z. P.; Anthiss, J. W.; Staples, R. J. *Inorg. Chem.* **2002**, *41*, 278–286. (d) Miao, Y. L.; Liu, J. L.; Leng, J. D.; Lin, Z. J.; Tong, M. L. *CrystEngComm* **2011**, *13*, 3345–3348.
- (7) (a) Miao, Y. L.; Liu, J. L.; Li, J. Y.; Leng, J. D.; Ou, Y. C.; Tong, M. L. *Dalton Trans.* **2011**, *40*, 10229–10236. (b) Guo, Y. N.; Xu, G. F.; Guo, Y.; Tang, J. K. *Dalton Trans.* **2011**, *40*, 9953–9963.
- (8) (a) Jiang, S. D.; Wang, B. W.; Su, G.; Wang, Z. M.; Gao, S. *Angew. Chem., Int. Ed.* **2010**, *49*, 7448–7451. (b) Vitali, L.; Fabris, S.; Conte, A. M.; Brink, S.; Ruben, M.; Baroni, S.; Kern, K. *Nano Lett.* **2008**, *8*, 3364–3368. (c) Ishikawa, N.; Sugita, M.; Wernsdorfer, W. *J. Am. Chem. Soc.* **2005**, *127*, 3650–3651.
- (9) (a) Gao, Y. J.; Xu, G. F.; Zhao, L.; Tang, J. K.; Liu, Z. L. *Inorg. Chem.* **2009**, *48*, 11495–11497. (b) Rinck, J. L.; Novitchi, G.; Heuvel, W. V.; Ungur, L.; Lan, Y. H.; Wernsdorfer, W.; Anson, C. E.; Chibotaru, L. F.; Powell, A. K. *Angew. Chem., Int. Ed.* **2010**, *49*, 7583–7587. (c) Mori, F.; Nyui, T.; Ishida, T.; Nogami, T.; Choi, K. Y.; Nojiri, H. *J. Am. Chem. Soc.* **2006**, *128*, 1440–1441.
- (10) Spek, A. L. *PLATON, A Multipurpose Crystallographic Tool*; Utrecht University: Utrecht, The Netherlands, 1998.
- (11) (a) Poneti, G.; Bernot, K.; Bogani, L.; Caneschi, A.; Sessoli, R.; Wernsdorfer, W.; Gatteschi, D. *Chem. Commun.* **2007**, *18*, 1807–1809. (b) Sessoli, R.; Powell, A. K. *Coord. Chem. Rev.* **2009**, *253*, 2328–2341.
- (12) Tang, J.; Hewitt, I.; Madhu, N. T.; Chastanet, G.; Wernsdorfer, W.; Anson, C. E.; Benelli, C.; Sessoli, R.; Powell, A. K. *Angew. Chem., Int. Ed.* **2006**, *45*, 1729–1733.
- (13) (a) Gatteschi, D.; Sessoli, R. *Angew. Chem., Int. Ed.* **2003**, *42*, 269–297. (b) Gatteschi, D.; Sessoli, R.; Villain, J. *Molecular Nanomagnets*; Oxford University Press: Oxford, U.K., 2006.
- (14) (a) Zhou, Q.; Yang, F.; Xin, B. J.; Zeng, G.; Zhou, X. J.; Liu, K.; Ma, D.; Li, G. H.; Shi, Z.; Feng, S. H. *Chem. Commun.* **2013**, *49*, 8244–8246. (b) Biswas, S.; Jena, H. S.; Adhikary, A.; Konar, S. *Inorg. Chem.* **2014**, *53*, 3926–3928.
- (15) (a) Xue, S.; Zhao, L.; Guo, Y.; Zhang, P.; Tang, J. *Chem. Commun.* **2012**, *48*, 8946–8948. (b) Wang, H.; Liu, T.; Wang, K.; Duan, C.; Jiang, J. *Chem.—Eur. J.* **2012**, *18*, 7691–7694.